Supplementary Information (SI) for Chemical Communications.

Electronic Supplementary Information

Dual-Functional Structural Modulation for Stabilizing Sodium Layered Oxide Cathodes

Qiang Ma,[a #] Qingqun Sun,[b #] Jingqiang Wang*[c] Qicong Ling,[b] Ruizi Li,[b] Mengying Li,[b] Zhuangchun Jian,[b] Dixing Ni,*[d] Haodong Wang,[c] Yafang Wang,[a] Yanfang Zhu*[b] and Yao Xiao*[b]

[a] College of Materials Engineering, Henan International Joint Laboratory of Rare Earth Composite Materials, Henan Key Laboratory of Electronic Ceramic Materials and Application, Henan University of Engineering, Zhengzhou, Henan 451191, P. R. China.

[b] College of Chemistry and Materials Engineering, Wenzhou University, Wenzhou, 325035, China. E-mails: yanfangzhu@wzu.edu.cn, xiaoyao@wzu.edu.cn.

[c] College of Chemistry and Chemical Engineering, Inner Mongolia University, Hohhot, Inner Mongolia, 010021, China. E-mails: wjq@imu.edu.cn,

[d] High Performance Computing Department, National Supercomputing Center in Shenzhen, Shenzhen, Guangdong 518055, China. nidx@nsccsz.cn

#Qiang Ma and Qingqun Sun contribute equally to this work.

Experimental

Material Synthesis

The $Na(Ni_{1/3}Fe_{1/3}Mn_{1/3})_{0.98}WB_{0.02}O_2$ cathode was synthesized by conventional solid-phase sintering method. The stoichiometric amounts of Na_2CO_3 (10% excess to compensate for sodium evaporation), NiO, Fe_2O_3, Mn_2O_3 and WB are thoroughly ground in agate mortar for 40min to make them evenly mixed and pressed into pellets under the pressure of 16 MPa. Subsequently, the pellets were sintered in a sintering furnace at a heating rate of 5 °C min^{-1} at 1000 °C in an air atmosphere for 15 h, and then naturally cooled to room temperature. For comparative study, a control sample composed of $Na(Ni_{1/3}Fe_{1/3}Mn_{1/3})_{1-x}WB_xO_2$ (x =0, 0.01, 0.03, 0.04) was synthesized under the same processing conditions.

Material Characterization

The microstructural morphology of as-prepared materials was characterized using scanning electron microscopy (SEM, SEM3100-CIQTEK). Phase identification of synthesized oxide cathodes was performed via X-ray diffraction (XRD, PANalytical) with Cu Kα radiation (λ = 1.5418 Å). High-resolution transmission electron microscopy (HR-TEM, FEI Talos F200) provided atomic-scale lattice information. Synchrotron radiation X-ray absorption spectroscopy (XAS) measurements were performed at the Australian Synchrotron's medium-energy X-ray beamlines (MEX1 and MEX2, beamtime IDs: M23254, M23262).

Electrochemistry

The cathodes were prepared by mixing the active material, Super P conductive carbon, and polyvinylidene difluoride (PVDF) binder in a 7:2:1 ratio in N-methyl-2-pyrrolidone (NMP) to form a uniform slurry. This mixture was coated onto Al foil and dried under vacuum at 80 °C overnight. The active material loading was approximately 2 mg cm^{-2}. The electrolyte consisted of 1 M $NaClO_4$ dissolved in propylene carbonate with 5 vol.% fluoroethylene carbonate as an additive. Metallic sodium was used as the counter electrode, and porous glass fiber acted as the separator. Coin cells (CR2032) were assembled in an argon-filled glove box, and galvanostatic charge-discharge testing was performed using a NEWARE Battery Test System. CV tests were conducted by an electrochemical workstation (CHI 760E).

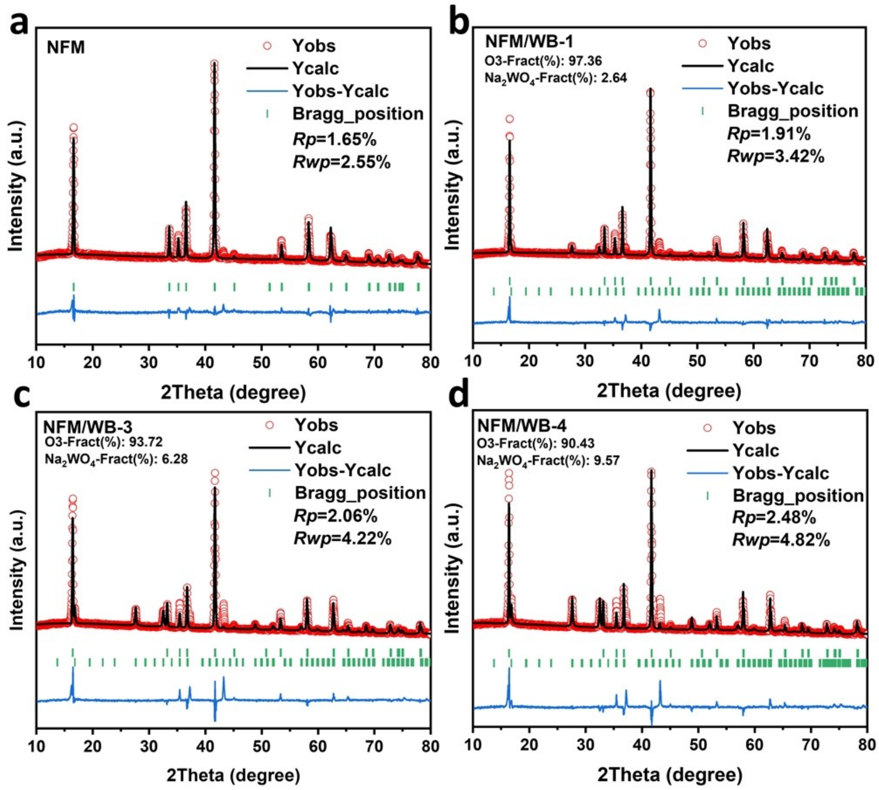

Figure S1. XRD patterns of (a) NFM, (b) NFM/WB-1, (c) NFM/WB-3, (d) NFM/WB-4.

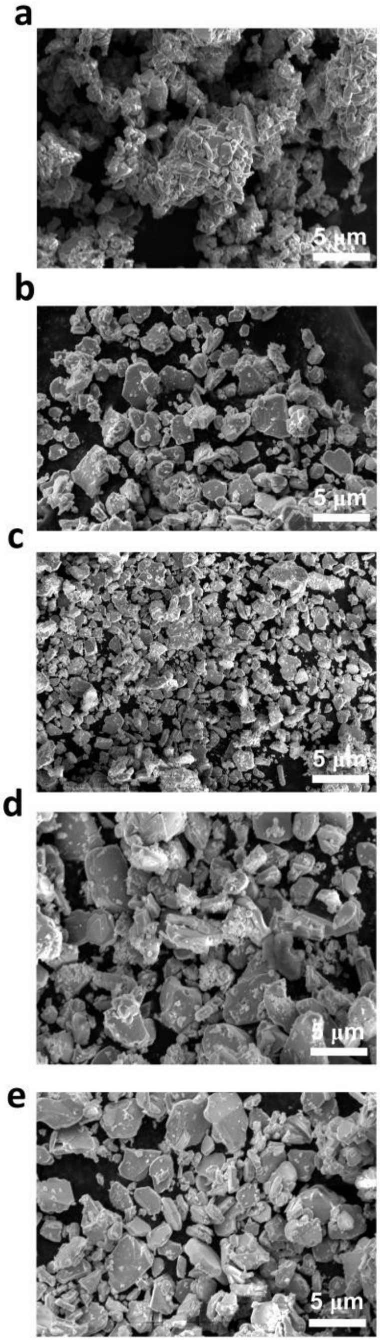

Figure S2. The SEM images of (a) NFM, (b) NFM/WB-1, (c) NFM/WB-2, (d) NFM/WB-3 and (e) NFM/WB-4.

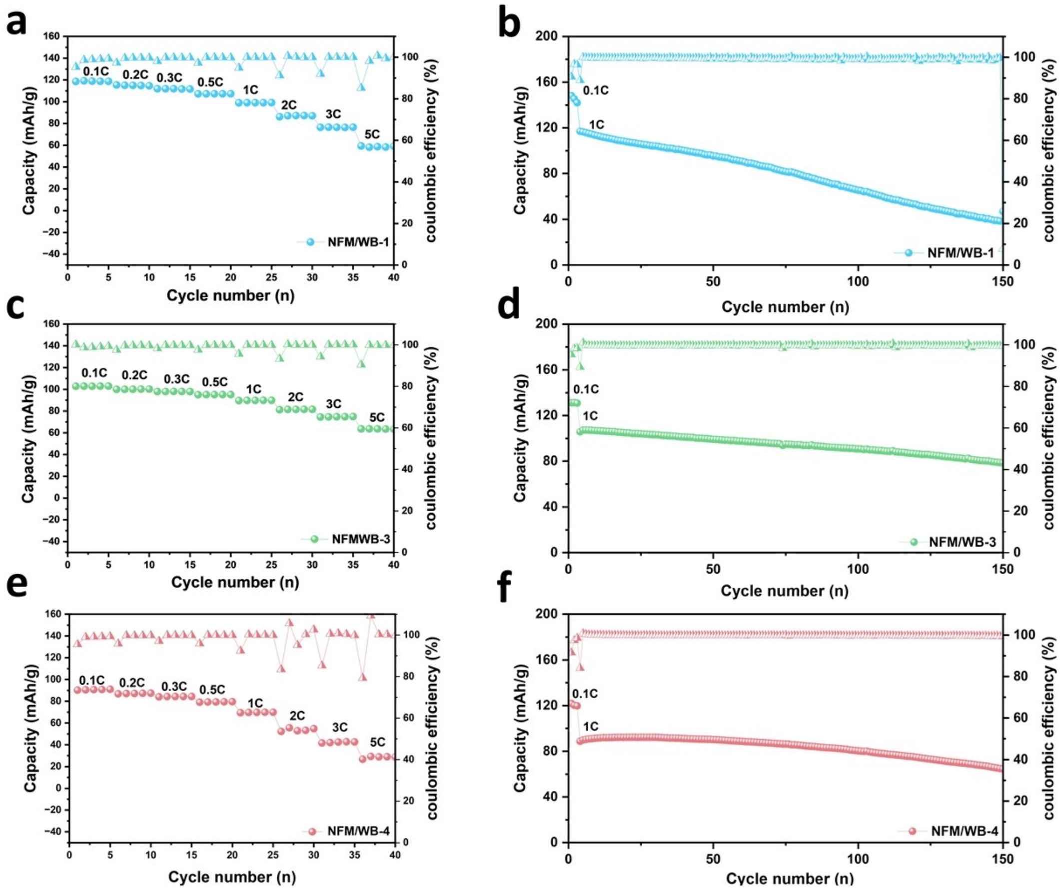

Figure S3. Rate and cycle performance of (a, b) NFM/WB-1, (c, d) NFM/WB-3 and (e, f) NFM/WB-4 at 0.1 C- 0.5 C and 1 C.

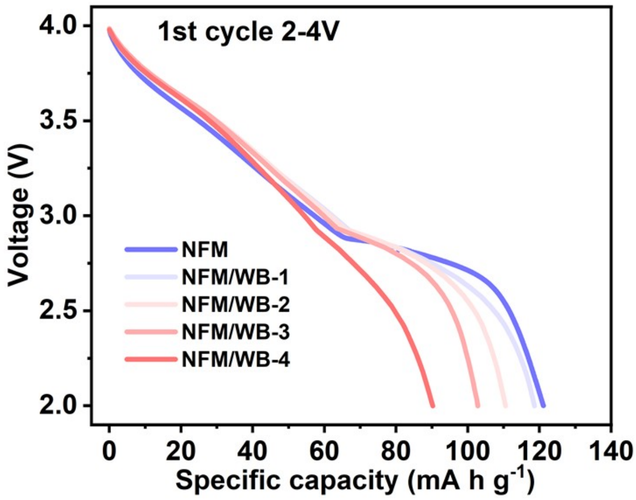

Figure S4. The first discharge curves of NFM, NFM/WB-1, NFM/WB-2, NFM/WB-3 and NFM/WB-4 in 2-4 V at 1 C.

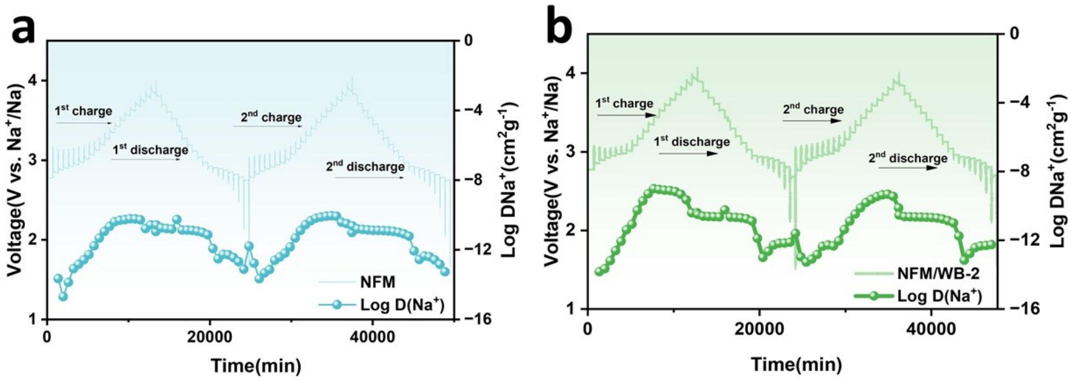

Figure S5. GITT curves and the corresponding Na-ions diffusion coefficient of the (a) NFM and (b) NFM/WB-2.

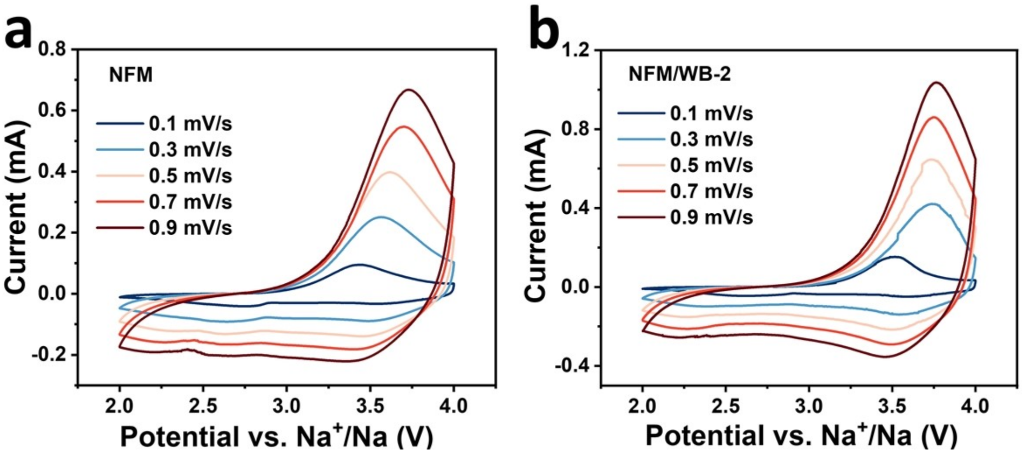

Figure S6. CV curves of the (a) NFM and (b) NFM/WB-2 at 0.1 mV/s, 0.3 mV/s, 0.5 mV/s, 0.7 mV/s and 0.9 mV/s.

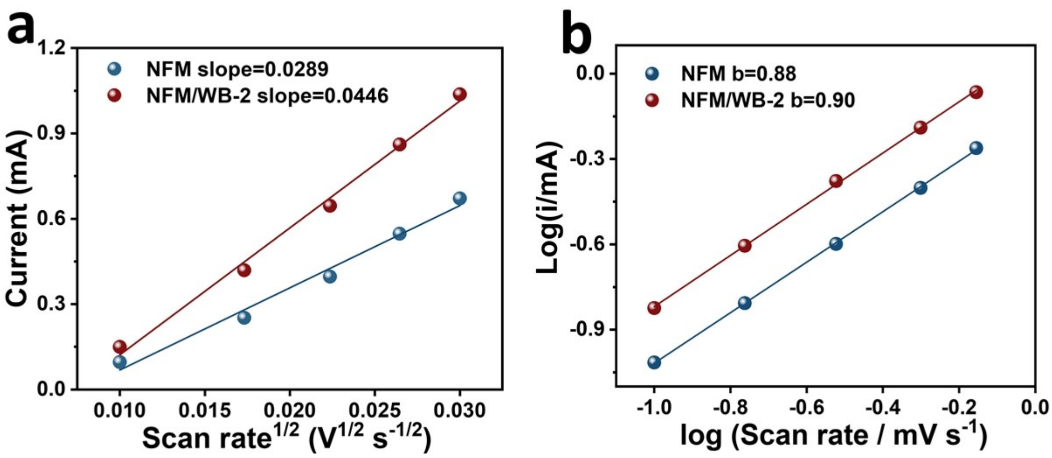

Figure S7. (a) Linear fitting of peak current versus square root of the scan rate, (b) Linear fitting of log (*i)* versus log (*v*) plots at oxidation peaks of NFM and NFM/WB-2, respectively.

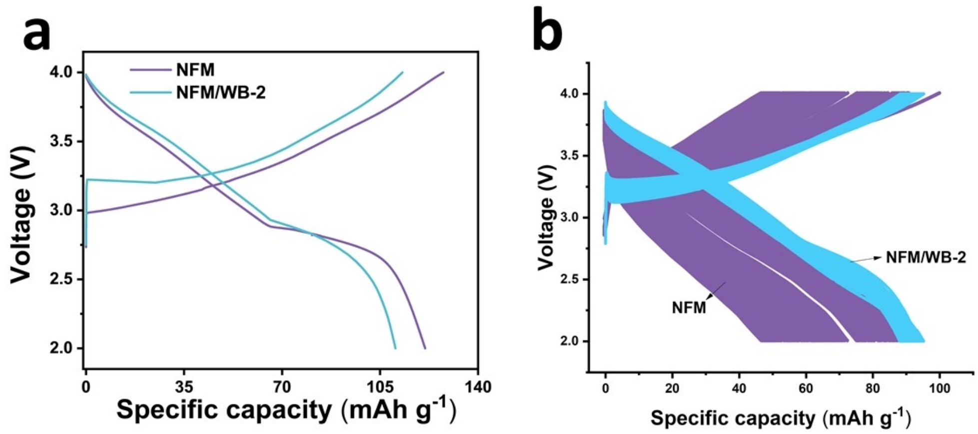

Figure S8. (a) Comparison of the first cycle performance of NFM and NFM/WB-2. (b) Charge-discharge curves of NFM and NFM/WB-2 from the 5th to 150th cycle in 2-4 V at 1 C.

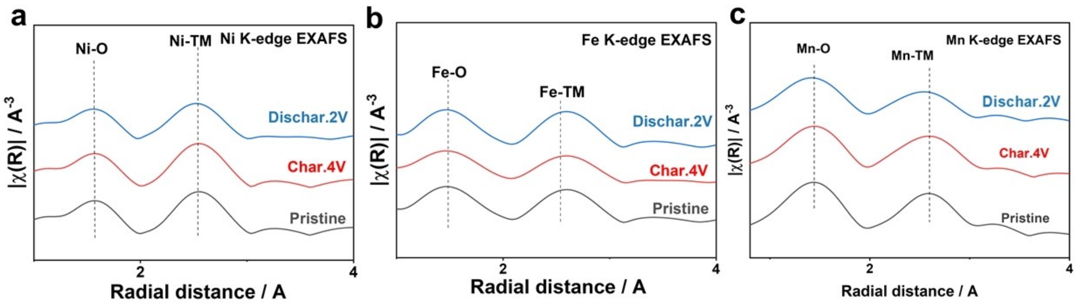

Figure S9. (a-c) K-edge ex situ EXAFS spectra of (a) Ni, (b) Fe, and (c) Mn in the NFM/WB-2 sample at pristine and charge/discharge state.

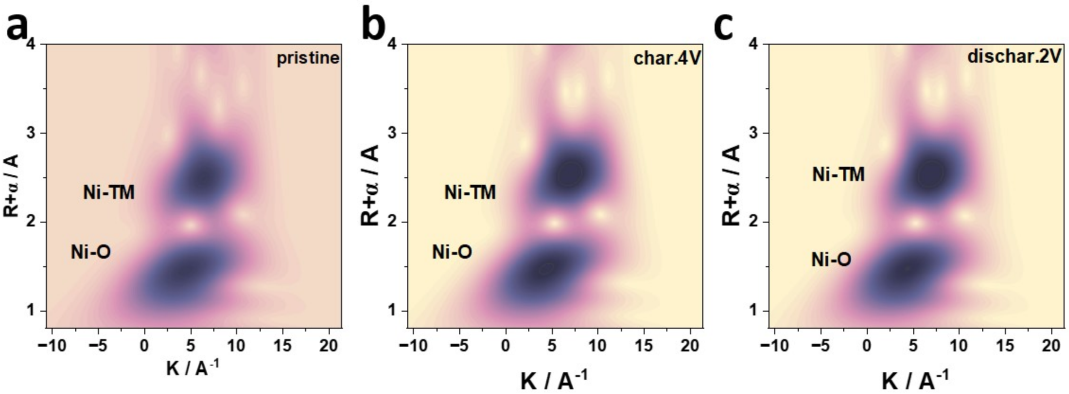

Figure S10. (a-c) Ni K-edge EXAFS WT images of NFM/WB-2 sample at pristine and charge/discharge.

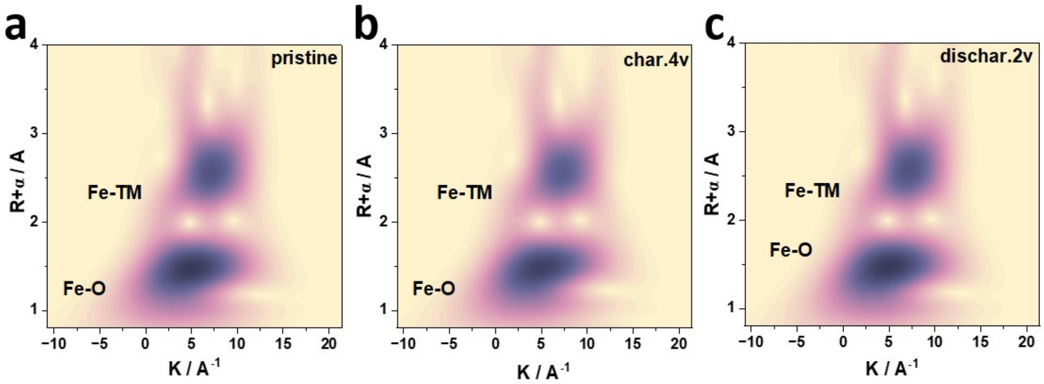

Figure S11. (a-c) Fe K-edge EXAFS WT images of NFM/WB-2 sample at pristine and charge/discharge state.

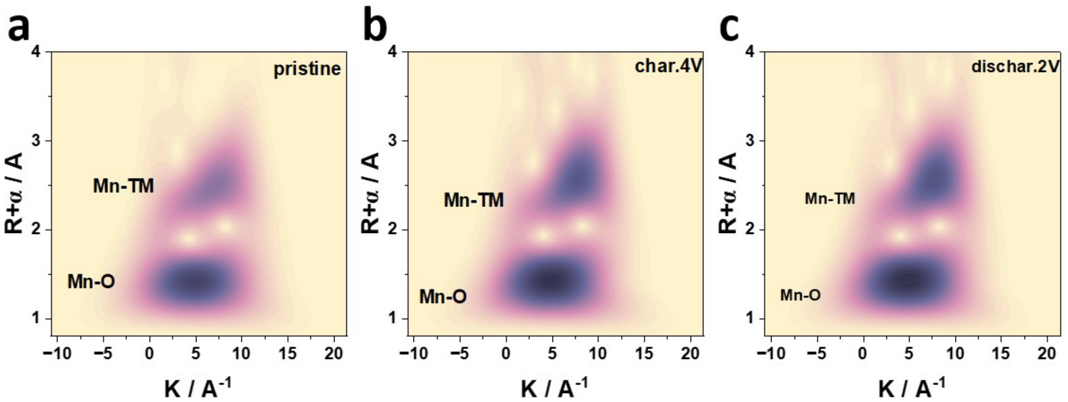

Figure S12. (a-c) Mn K-edge EXAFS WT images of NFM/WB-2 sample at pristine and charge/discharge.

Table S1. Unit cell parameters refined by XRD

Cell parameters(Å)	NFM	NFM/WB-1	NFM/WB-2	NFM/WB-3	NFM/WB-4
a	2.97985	2.97285	2.96590	2.96140	2.95885
b	2.97985	2.97285	2.96590	2.96140	2.95885
c	15.99946	16.07299	16.13388	16.18150	16.22577
Na_2WO_4 phase proportion	0%	2.64%	3.99%	6.28%	9.57%

Table S2. Comparison of electrochemical performance with the existing literature.

Cathodes	Specific capacity mAh/g	Cycle retention	References
Na_2WO_4-NFM	110@0.1C	96.5% after150 cycles @1C	This work
NFM-Cl	130@0.1C	89.10% after 200 cycles@1C	1
Al_2O_3@NFM	129.97@0.1C	87.75% after 100 cycles@0.5C	2
NFM@YDC-1%-	-	71.63% after 300 cycles@1C	3
$NaNi_{1/3}Fe_{1/3}Mn_{1/3}O_2$	129.9@0.1C	75% after 200 cycles@1C;	4
Gradient architecture $NaNi_{1/3}Fe_{1/3}Mn_{1/3}O_2$	145.2@0.1C	82.2% after 500 cycles@1C	5
$NaNi_{0.32}Fe_{0.32}Mn_{0.32}Al_{0.02}Cu_{0.02}O_2$	140@0.1C	81% after 200 cycles@1C	6
$NaNi_{1/3}Fe_{1/3}Mn_{1/3-0.02}Zr_{0.02}O_2$	125.6@0.1C	77.7% after 300 cycles@1C	7
NaNFMO-TW	123.3@0.1C	82.6% after 300 cycles@1C	8
SC-NFM	129@0.1C	83.1% after 350 cycles@1C	9
Y- $NaNi_{1/3}Fe_{1/3}Mn_{1/3}O_2$	120.8@0.1C	72.26% after 200 cycles@1C	10
Ca-NFM	135.5 @ 0.1C	76.8% after 500 cycles@1C	11
NNFMCe-2	123.1 @0.2C	86.5% after 100 cycles@1C	12

Reference

1. Z. Qiu, S. Li, W. Zhou, F. Liu, Y. Zhang, Y. Zhang, H. Wang, Y. Lai and Z. Zhang, *J. Energy Chem.*, 2025, **111**, 867-876.
2. M. Chen, C. Zhao, Y. Li, H. Wang, K. Wang, S. Yang, Y. Gao, W. Zhang, C. Chen, T. Zhang, L. Wen, K. Dai and J. Mao, *J. Energy Chem.*, 2025, **102**, 107-119.
3. W. Tang, Y. Li, S. Jiang, C. Lei and Z. He, *Chem. Eng. J.*, 2025, **525**, 170210.
4. W. Tang, Y. Li, S. Jiang, C. Lei and Z. He, *J. Energy Storage*, 2025, **128**, 117080.
5. Y. Liang, W. Liu, Z. Tang, M. Qin, J. Zeng and X. Wang, *Compos. Part B Eng.*, 2026, **309**, 113073.
6. S. Feng, C. Zheng, Z. Song, X. Wu, M. Wu, F. Xu and Z. Wen, *Chem. Eng. J.*, 2023, **475**, 146090.
7. C. Jiang, Y. Wang, Y. Xin, X. Ding, S. Liu, Y. Pang, B. Chen, Y. Wang, L. Liu, F. Wu and H. Gao, *Carbon Neutraliz.*, 2024, **3**, 233-244.
8. Z. Qin, Y. Liu, Y. He, P. Wang, G. Zhao, H. Yao, Y. Lin, Z. Huang and J. Li, *ACS Appl. Mater. Interfaces*, 2025, **17**, 7629-7640.
9. M. Yang, Z. Fan, J. Liu, Y. Ma, Y. Bai, X. Wang, H. Zhang, F. Hai, W. Hua, Y. Ma, Y. Wu and W. Tang, *Energy Fuels*, 2024, **38**, 2453-2462.
10. W. Tang, Y. Liu, C. Lei, Y. Li and Z. He, *Ionics*, 2024, **30**, 7027-7036.
11. Z. Yang, J. Xie, Y. Li, Y. He, G. Liu, G. Qu, G. Zhang, Y. Wang, J. Zhou, Y. Huang and C. Wang, *J. Am. Chem. Soc.*, 2025, **147**, 44060-44071.
12. Y. Li, L. Lei, J. Hou, G. Wang, Q. Ren, Q. Shi, J. Wang, L. Chen, G. Zu, S. Li, J. Wu, Y. Xu and Y. Zhao, *J. Energy Chem.*, 2025, **105**, 224-232.